Extended Abstracts of the 2005 International Conference on Solid State Devices and Materials, Kobe, 2005, pp.208-209

I-1-4

# Enhanced Breakdown Characteristic of AlGaN/GaN HEMTs Using a Gate/Drain Double Field-Plate Structure

Seunghun Kim and Kyounghoon Yang

Division of Electrical Engineering, Dept. of Electrical Engineering and Computer Science (EECS),
Korea Advanced Institute of Science and Technology (KAIST),
373-1, Guseong-dong, Yuseong-gu, Daejeon, Republic of Korea
Phone: +82-42-869-5471, Fax: +82-42-869-8021, E-mail: khyang@ee.kaist.ac.kr

## 1. Introduction

AlGaN/GaN HEMTs have played an important role in microwave and millimeter-wave power applications due to the excellent characteristics, such as a wide bandgap, a high breakdown field, a high saturation velocity and a high thermal conductivity [1]. In order to improve device power performance, increasing of the breakdown voltage is needed. Hence, various technologies have been developed [2]-[6]. Especially, field-plate (FP) structures have been widely used to reduce the gate edge electric field, which lead to high breakdown voltages [6], [7]. Recently, Saito et al. used a source/drain double field-plate (DFP) structure in the AlGaN/GaN HEMT to suppress the edge electric field between the extended source and drain contacts, demonstrating significant improvement in the device breakdown characteristics for low frequency switch applications [8].

In this work, we propose a new DFP structure implemented at the gate and drain sides of the AlGaN/GaN HEMT for microwave applications. Significantly improved breakdown characteristics have been obtained from the proposed device structure.

## 2. Device Structure and Fabrication

The fabricated AlGaN/GaN HEMT structure is shown in Fig. 1. The device structure was grown by metal-organic chemical vapor deposition (MOCVD) and consists of a sapphire substrate, a 400 Å AlN nucleation layer, a 3 μm undoped GaN buffer layer, and a 300 Å undoped $Al_{0.3}Ga_{0.7}N$ barrier layer. The device fabrication starts with device isolation, which is achieved by remote ion beam etching (RIBE) using $Ar\text{-}Cl_2$ gases with an etching rate of 400 Å/min for the GaN material. The drain and source ohmic contacts were formed using Ti/Al/Ti/Au (150/1000/450/550 Å) metals, which were evaporated and annealed at 850 °C for 30 sec in $N_2$ ambient. A contact resistance of 0.34 Ω·mm was obtained from the standard TLM measurement. The gate Schottky contact was formed by evaporating Ni/Au (200/3000 Å). The devices were then passivated by a 1000 Å-SiN film using remote plasma chemical vapor deposition (RPCVD). Finally, the DFP was formed by evaporating Ti/Au (150/3000 Å) on top of the passivation film. The proposed DFP structure consists of two FPs; one is a plate extended from the gate metal contact and the other is extended from the drain metal contact over the passivation layer as shown in Fig. 1. In order to investigate the effects of the proposed DFP structure, the devices with the conventional gate FP structure, which does not have the drain-side FP, were simultaneously fabricated as a reference device.

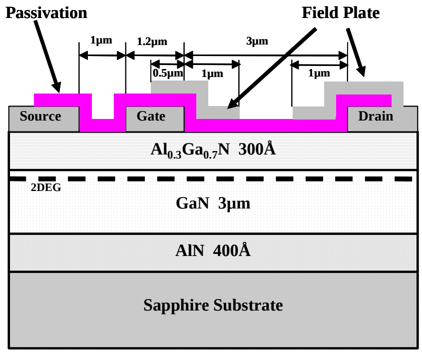


Fig. 1. AlGaN/GaN HEMT with the proposed DFP

Gate-source and gate-drain spacings of the fabricated devices were 1 μm and 3 μm, respectively. The gate width and length of the devices were 100 μm and 1.2 μm, respectively. Details on the DFP dimensions are shown in Fig. 1.

## 3. Device DC and RF Performance

The DC I-V characteristics of the fabricated devices are shown in Fig. 2. Both devices showed good channel pinch-off characteristics up to the drain to source voltage ($V_{ds}$) of 15V at the gate to source voltage ($V_{gs}$) of -5V. As shown in Fig. 2, the maximum drain to source current ($I_{ds,max}$) is 661mA/mm for the DFP structure and 660 mA/mm for the FP structure at $V_{gs}$ = 1V. The measured DC transconductances ($g_m$) are shown in Fig. 3. The peak transcoductance ($g_{m,peak}$) is 159mS/mm for the DFP structure and 156mS/mm for the FP structure at $V_{ds}$ = 3V. From the DC measurement results, it is found that the proposed DFP structure shows similar DC characteristics

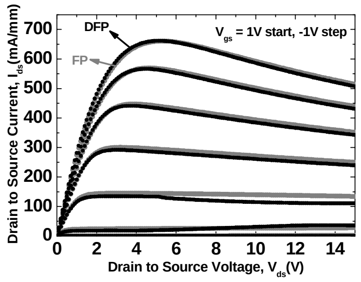


Fig. 2. Measured DC I-V characteristics for the DFP and FP HEMTs.

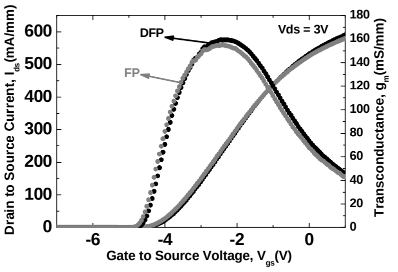


Fig. 3. Measured DC transconductance characteristics for the DFP and FP HEMTs.

| | DFP | FP |
|---|---|---|
| $f_T$ (GHz) | 6.4 | 6.8 |
| $f_{MAX}$ (GHz) | 15.3 | 16.8 |
| $C_{gs}$ (fF) | 337.6 | 334.1 |
| $C_{gd}$ (fF) | 49.1 | 42.8 |

Table. 1. Comparison of RF characteristics and small-signal parameters for the DFP and FP HEMTs.

compared to the FP structure without any degradation of DC performance.

The small-signal microwave characteristics were measured on wafer. The peak $f_T$ (maximum current-gain cutoff frequency) and $f_{MAX}$ (maximum oscillation frequency) are shown in Table. 1. The peak $f_T$ and $f_{MAX}$ are 6.4 GHz and 15.3 GHz for the DFP structure and 6.8 GHz and 16.8 GHz for the FP structure, respectively. From the measured results, the peak $f_T$ and $f_{MAX}$ of the DFP structure are observed to be slightly decreased compared to the FP structure. In order to characterize the measured results, the small-signal equivalent-circuit parameters were extracted from the measured S-parameters for the two structures. The results are summarized in Table. 1. As shown in Table. 1, the gate-source and gate-drain capacitances in the DFP structure are slightly increased compared to the FP structure due to the presence of the drain-side FP, which result in the slightly decreased cutoff frequencies.

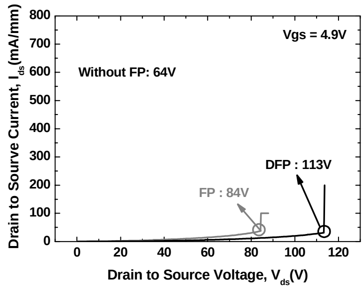


Fig. 4. Measured breakdown characteristics for the DFP and FP HEMTs.

The off-state breakdown characteristics are measured and compared in Fig. 4. As shown in Fig. 4, the breakdown voltage is improved from 84V for the FP structure to 113V for the proposed DFP structure, demonstrating 35% improvement of the breakdown voltage. This result indicates that the proposed DFP structure can significantly improve the device breakdown characteristics compared to the typical single gate FP structure, which means that the proposed DFP structure is very promising for high-power operation of the device.

## 4. Conclusion

The DC and RF small-signal performances of the proposed DFP HEMT have been measured and compared with those of the conventional FP HEMT.

The measurement results show that the DFP structure exhibits similar DC and RF small-signal gain characteristics with significantly improved breakdown characteristics, when compared to the single gate FP structure. These results demonstrate that the new DFP structure proposed in this work is very attractive for microwave power applications.

## Acknowledgement

This work was supported by KOSEF under the ERC program through the MINT Research Center at Dongguk University in the Republic of Korea.

## Reference

[1] U. K. Mishra, et al., Proceeding of IEEE, vol. 90, pp. 1022- 1031, 2002.
[2] L. W. Yin, et al., IEEE Electron Device Lett., vol. 11, pp. 561-563, 1990.
[3] J. C. Huang, et al., IEEE Trans. Microwave Theory Tech., vol. 41, pp. 752-759, 1993.
[4] C. L. Chen, et al., IEEE Electron Device Lett., vol. 13, pp. 335-337, 1992.
[5] P. K. T. Mok, et al. IEEE Trans. Electron Devices, vol. 41, pp. 246-250, 1994.
[6] K. Asano, et al., IEDM Tech, Dig., pp. 59-62, 1998.
[7] A. Chini, et al., IEE Electronics Lett., vol. 40, pp. 73-74, 2004.
[8] W. Saito, et al. IEEE Trans. Electron Devices, vol. 52, pp. 106-111, 2005.